

Characterization of FeCo based catalyst for ammonia decomposition. The effect of potassium oxide

Zofia Lendzion-Bieluń*, Rafał Pelka, Łukasz Czekajło

West Pomeranian University of Technology, Szczecin, Institute of Inorganic Chemical Technology and Environmental Engineering, Poland, Pułaskiego 10, 70-322 Szczecin,

*Corresponding author: zosi@zut.edu.pl

This article is dedicated to Professor Walerian Arabczyk on the occasion of his 70th birthday.

FeCo fused catalyst was obtained by fusing iron and cobalt oxides with an addition of calcium, aluminium, and potassium oxides (CaO, Al₂O₃, K₂O). An additional amount of potassium oxide was inserted by wet impregnation. Chemical composition of the prepared catalysts was determined with an aid of the XRF method. On the basis of XRD analysis it was found that cobalt was built into the structure of magnetite and solid solution of CoFe₂O₄ was formed. An increase in potassium content develops surface area of the reduced form of the catalyst, number of adsorption sites for hydrogen, and the ammonia decomposition rate. The nitriding process of the catalyst slows down the ammonia decomposition.

Keywords: ammonia decomposition, hydrogen, FeCo catalyst.

INTRODUCTION

Intensive investigations over hydrogen usage as a source for energy production are being conducted currently. Hydrogen application encompasses energy production in fuel cells, in stationary as well as portable devices. The fuel cells applications in transport means seem to be especially promising¹. Hydrogen production in the ammonia decomposition reaction has some advantages in comparison with conventional methods as steam reforming, coal gasification, and biomass catalytic gasification. First of all hydrogen from the ammonia decomposition contains no CO_x, which have poisoning impact on catalysts for fuel cells². Liquid ammonia may be easier stored than hydrogen¹. Infrastructure for ammonia production is developed very well and technology of ammonia is well known.

Taking into consideration ammonia decomposition thermodynamics it is a convenient process. At 400°C, under 1 atm. equilibrium degree reaches a value above 99%³. The ammonia decomposition reaction is being studied intensively to find new systems of active catalysts.

Previous investigations showed that elements from group VIII (Ru, Fe, Co, Ni, Ir, Rh)^{3, 4, 5, 6, 9} and carbides/nitrides^{7, 8} of molybdenum, vanadium, and tungsten catalyses ammonia decomposition reaction into hydrogen and nitrogen. Supported ruthenium catalysts show the highest activity in the ammonia decomposition reaction³. Limited availability of noble metals and a relatively low activity of non-noble metals induce to further works on optimization of catalytic systems for ammonia decomposition working at lower temperatures. The rate determining step of ammonia decomposition is the recombinative desorption of nitrogen atoms (i.e., N* + N* → N₂ + 2*)^{10, 11}. Iron binds nitrogen atoms strongly, iron catalyst surface saturates itself what finally, especially at lower temperatures, leads to a kind of poisoning¹². Ammonia decomposition rate depends on a degree of nitrogen saturation of the iron surface. Both theoretical^{5, 10, 11} and experimental studies¹³ show that bimetallic systems are promising catalysts for that reaction. The fundamental rule of that idea is to bind together two metals with opposite affinity towards nitrogen atoms e.g. Co-Mo¹⁴, Ni-Mo¹⁶, Ni-Pt¹⁰ or FeCo^{13, 17}.

For example the bimetallic Co-Mo catalyst supported on the MCM-41 carrier has a higher activity in the ammonia decomposition reaction than Co or Mo monometallic catalysts on the same carrier¹⁴. The same results were obtained in the work¹⁵ in which Co-Mo alloy was supported on γ-Al₂O₃ carrier what points to synergistic effect between Co and Mo. Addition of Mo may increase a dispersion of Co nanoparticles. Besides the dispersion of nanoparticles over the support surface the stability of nanoparticle has an important significance under catalyst working conditions. The authors of the work¹⁷ claimed that the stability of Co was significantly improved by alloying with Fe over carbon nanotubes. Moreover they pointed out that the sort of support is essential. During the thermal treatment or under reaction conditions reaction between nanoparticles of metal phase and oxides of support may take place. As a result the less reducible ternary oxide with spinel structure, having impact on the activity, may be formed. The observed changes in the activity are probably connected with the changes of the active sites on the catalyst surface. It was also found that an addition of Co into the Fe catalyst lowers the activation energy of the ammonia decomposition reaction in comparison with pure iron. The activity of catalysts in the ammonia decomposition reaction is connected with a sort and content of promoters. Special role is played by electron-donor promoters such as potassium³, caesium¹⁸ or barium¹⁹. In the studies¹⁸ it was presented that an increase in caesium content in ruthenium/nanotubes catalyst had caused an increase in ammonia decomposition degree and an decrease in the activation energy.

In this paper the impact of potassium oxide content on structural and catalytic properties of FeCo catalyst is presented. Distribution of nanocrystallites size in the reduced form of the catalyst, made according to the previously elaborated method based on measurements of the rate of the nitriding reaction of the catalyst, is presented.

EXPERIMENTAL

FeCo fused catalyst was obtained by fusing magnetite with an addition of calcium, aluminium, and potassium

oxides (CaO, Al₂O₃, K₂O). During the melting process cobalt(II, III) oxide was added. The prepared alloy of the catalyst was crushed and formed grains of the diameter in the range from 1.0 to 1.2 mm were separated for tests. Chemical compositions of the catalyst was determined with the aid of the X-ray fluorescence method (XRF) using Panalytical spectrometer, non-standards Omnia method was applied. XRD method was applied to identify catalyst phase composition before and after tests (Philips X'Pert Pro). Measurements of the specific surface area of the catalyst in the reduced form, using a single-point BET method, and temperature programmed desorption of hydrogen (TPD-H₂), were performed with an AutoChem II 2920 Micromeritics apparatus equipped with TCD. Before tests samples were being reduced with hydrogen at 600°C by 16 hours. Before TPD-H₂, the samples were first cooled to the room temperature in argon at the flow rate of 70 ml/min. Next, they were treated at 20°C for 40 minutes in hydrogen and then they were flushed with argon at the rate of 70 ml/min for 1 h to eliminate the physically adsorbed hydrogen. Finally, the samples were heated at a rate of 20°C/min in argon to record the TPD spectra.

In order to increase a content of potassium in the catalyst, catalyst was impregnated with water solution of KOH. Before the impregnation process, the catalyst was reduced. The reduction process was carried out at hydrogen atmosphere (99.999%) from 20 to 600°C with a heating rate of 15°C/min under ambient pressure.

A series of kinetic measurements of the nitriding process was made for 100% ammonia at a reactor inlet and next nitrides reduction with pure hydrogen at 400°C. Results of these measurements were used to determine a size distribution of the crystallites with a chemical method described in a paper²⁰. This method allows to determine a size distribution of crystallites of the reduced form of the catalysts.

Activity tests of the catalyst in the ammonia decomposition reaction were carried out in a differential reactor connected with thermogravimeter. Some 0.5 g of the oxidized catalyst of granulation of 1.0–1.2 mm was placed in a platinum basket as a monolayer bed. Before the ammonia decomposition and the nitriding tests, catalyst was reduced with pure hydrogen at 600°C. Measurements of catalysts activity were performed in the temperature range from 400 to 600°C under ambient pressure. The ammonia decomposition reaction was tested in the range of ammonia concentration at the reactor inlet from 0 to 100%. Total gas flow was constant – 200 sccm.

Changes of the gas phase, ratio NH₃/H₂, at the reactor inlet were made after reaching a stationary state and when all tests at these conditions were made. Gas phase content changes at the reactor inlet were made to change the value of the nitriding potential $P = p_{\text{NH}_3} / p_{\text{H}_2}^{1.5}$ at the reactor.

The concentration of hydrogen at the outlet of the reactor was measured on the basis of the thermal conductivity of gas and the concentration of hydrogen assuming stoichiometric decomposition of ammonia at the stationary state⁶. Conversion degree of ammonia α_{NH_3} was calculated from an equation 1.

$$\alpha_{\text{NH}_3} = \frac{X_{\text{H}_2} F^{\circ} - F_{\text{H}_2}^{\circ}}{F_{\text{NH}_3}^{\circ} (1.5 - X_{\text{H}_2})} \quad (1)$$

Where: F° – total gaseous reactants flow at the reactor inlet, mol · s⁻¹, $F_{\text{H}_2}^{\circ}$ and $F_{\text{NH}_3}^{\circ}$ – hydrogen and ammonia flows at the reactor inlet, mol · s⁻¹, X_{H_2} – molar concentration of hydrogen in the reactor, mol · mol⁻¹.

On the basis of degree of ammonia decomposition under given conditions of temperature and ammonia flow rate at the reactor inlet the rate of the ammonia decomposition reaction, related to mass of catalyst, was calculated from an equation 2.

$$r_{\text{decomp}} = \alpha_{\text{NH}_3} \times F_{\text{NH}_3}^{\circ} / m_{\text{cat}} \quad (2)$$

Where: α_{NH_3} – degree of ammonia decomposition, $F_{\text{NH}_3}^{\circ}$ – ammonia flow in the reactor inlet, mol · s⁻¹, m_{cat} – mass of catalyst, g.

A gas phase analysis and changes taking part in the solid phase during the ammonia decomposition process were being observed simultaneously.

RESULTS AND DISCUSSION

Chemical composition of the catalyst obtained in the melting process was determined with XRF method and was as follows: 1.05 wt% Al₂O₃, 1.23 wt% CaO, 0.21 wt% K₂O, 4.8 wt % Co₃O₄. The rest was composed of iron oxide Fe₃O₄. As a result of potassium hydroxide impregnation two additional catalysts were prepared with potassium oxide content of 0.47 wt. % and 0.87 wt. % respectively. In that way three catalysts varying one another of potassium oxide content, what was included into the catalyst names FeCo(0.21), FeCo(0.47), FeCo(0.87), were prepared.

On the basis of XRD analysis, Fig. 1, it was found that cobalt atoms were built into magnetite structure forming a solid solution. X-ray peaks were attributed to CoFe₂O₄ phase according to the JCPDS (01-077-0426) card.

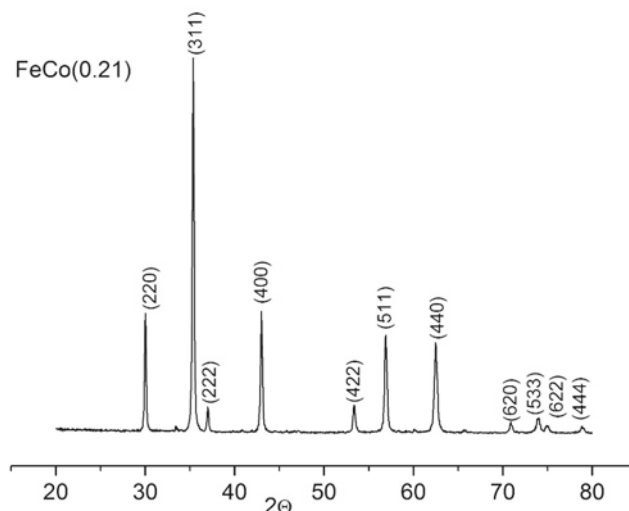


Figure 1. X-ray pattern of the oxidized form of the FeCo(0.21) catalyst

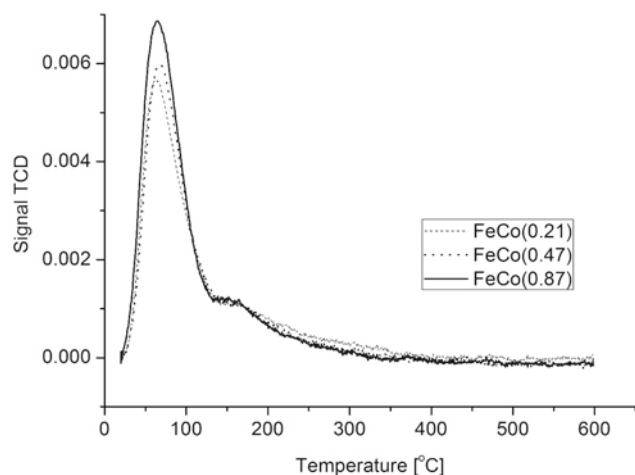
An insert of additional amount of potassium oxide into the system did not have an influence on a phase content of the catalysts, X-ray patterns were not presented.

Specific surface areas of the reduced forms of the catalysts and volumes of desorbed hydrogen after TPD-H₂ process were showed in Table 1. The specific surface of the reduced catalysts increase while potassium oxide content rises. The increase in the specific surface area influences on a sorption of hydrogen.

Table 1. Specific surface area of the catalysts in the reduced form and volume of adsorbed hydrogen in the TPD-H₂ process

Catalyst	S _{BET} [m ² /g _{cat}]	V _{H₂} [cm ³ /g _{cat}]
FeCo(0.21)	10.50	0.3085
FeCo(0.47)	11.28	0.3111
FeCo(0.87)	12.49	0.3154

Changes of katharometer signal, connected with changes of hydrogen content and temperature for catalysts with various content of potassium oxide are presented in Figure 2.

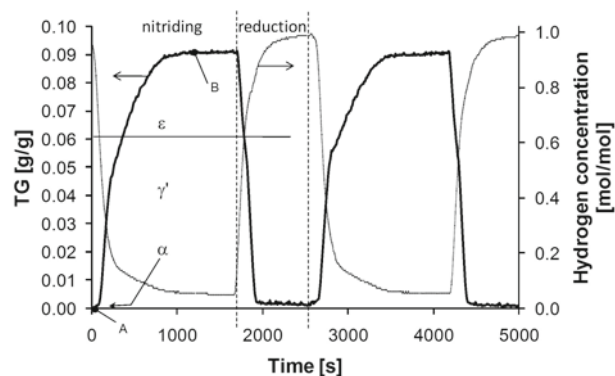
**Figure 2.** TPD-H₂ of the catalysts modified with potassium

Two maxima were observed on the curve of TPD-H₂, the first one at about 66°C and the second one at about 165°C. With the increase in the K₂O content in the catalyst number of active adsorption sites for hydrogen with weaker bond energy on the catalyst surface increases too.

Results of measurements of nitriding degree of FeCo(0.21) catalyst in the nitriding process (ammonia of 100% at the reactor inlet, temperature of 400°C) and nitrides reduction were showed in Figure 3. The nitriding runs at these conditions for other catalysts were not showed because no important differences had been registered. Nitriding degree, m_N , was defined as a ratio of nitrogen mass at the given moment of the process to mass of metallic phase of α -FeCo, m_{FeCo} . In the plot changes of hydrogen content in the gas phase during the reaction were also presented. Contents of the others components of gas phase were determined on the basis of the reactor mass balance.

An observed mass change of the catalyst, 0.003 g/g, in the initial stage (about 100 s), was connected with a nitrogen dissolution in the metallic phase of α -(FeCo). In the next stage an increase in mass runs until reaching an inflection point at $m_N = 0.053$ g/g connected with formation of γ' -(FeCo)₄N phase and its saturation with nitrogen. Above that level a new phase, ϵ -(FeCo)₃N, comes into being. Mass stabilization takes place at $m_N = 0.09$ g/g. Stationary state was settled, in which mass of the catalyst and gas phase composition are constant. Next, obtained nitrides were reduced with hydrogen.

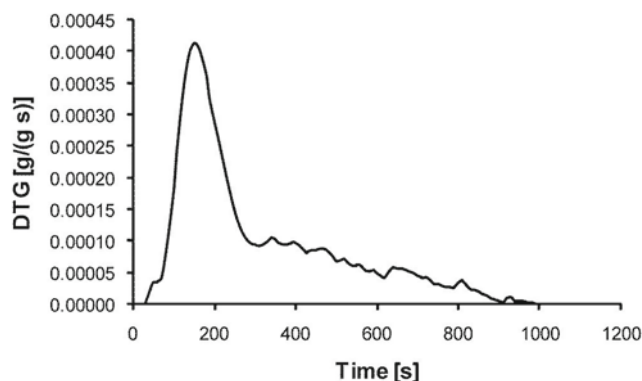
Nitriding degree and shapes of TG curves obtained in several cycles (on the plot only two cycles are presented, in fact many cycles were carried out) are the same, what

**Figure 3.** Thermogravimetric curve and changes of hydrogen content determined for nitriding process of the alloy FeCo(0.21) catalyst (ammonia content at the reactor inlet – 100%, temperature – 400°C)

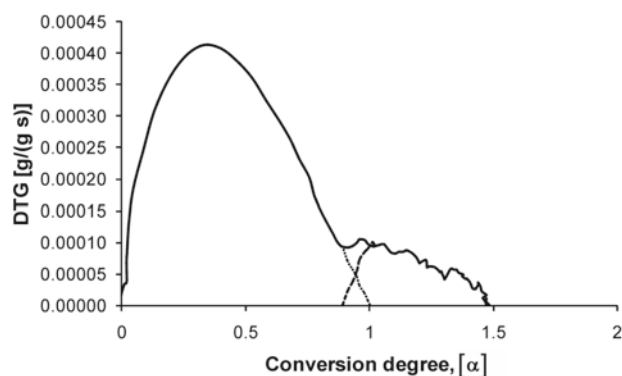
indicates to catalyst structure stability during the run of experiment.

Analysing the nitriding process, it can be noticed that mass of the sample and gas phase composition were stabilized after about 1000 s. During the reduction stabilization of the solid phase is very fast – 300 s, while gas phase needs more time to be stabilized, what is sometimes connected with gas exchange in the reactor.

After differentiating AB curve interval from Figure 3, the rate of nitriding process was determined (Fig. 4.).

**Figure 4.** Nitriding reaction rate (ammonia content at the reactor inlet – 100%, temperature – 400°C).

After transformation function from $DTG = f(t)$ into $DTG = f(\alpha)$ rates of forming γ' and ϵ phases were separated (Fig. 5). Conversion degree α defined as ratio of mass of bound nitrogen at given while of the reaction and mass of nitrogen in just forming γ' nitride phase.

**Figure 5.** Rate of nitriding reactions of α -FeCo into γ' phase and γ' phase into ϵ phase, (ammonia content at the reactor inlet – 100%, temperature – 400°C)

For further calculation data concerning the rate of γ phase forming were applied. The rate of the nitriding reaction as a function of nanocrystallites size distribution may be described by the following equation:

$$r_{\text{nit}} = k (P - P_0) f(\alpha)$$

k – nitriding reaction rate constant; P_0 – minimum nitriding potential required to start the nitriding reaction.

On the basis of the above equation and an assumption that specific surface area equals $10.5 \text{ m}^2/\text{g}$, distribution of nanocrystallites size was determined.

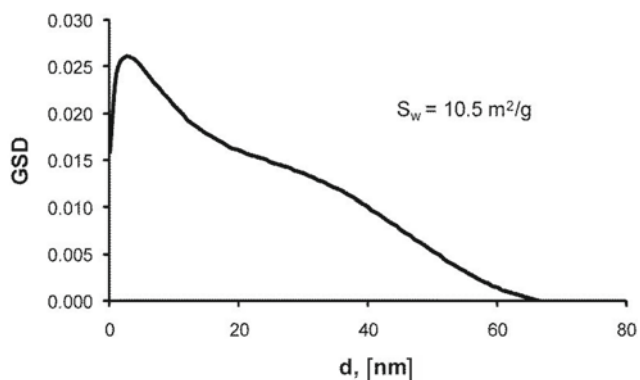
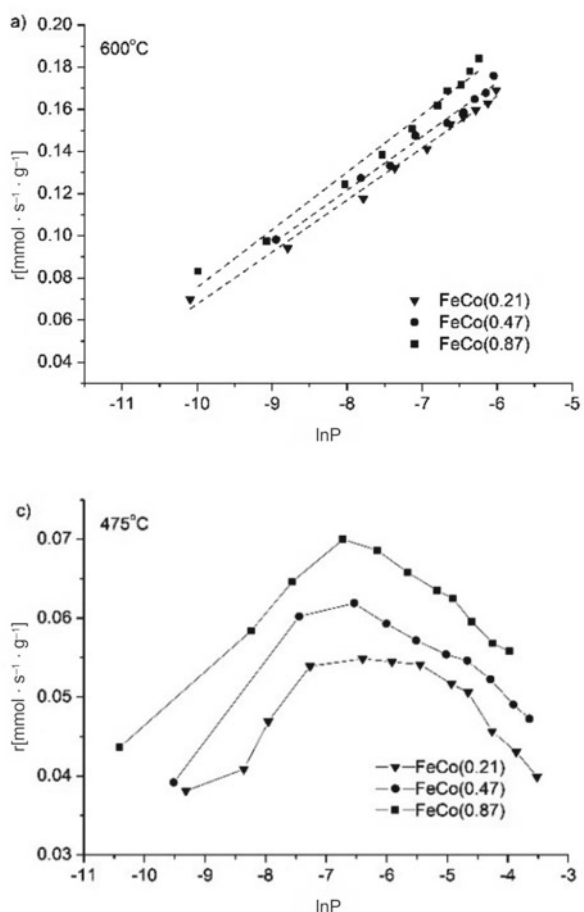


Figure 6. Distribution of nanocrystallites size of the reduced FeCo catalyst

From the distribution crystallites size showed in Figure 6 it was found that crystallites of various size are presented in the catalyst. Crystallites of about 5 nm size participate in the largest volume, next maximum is visible for 30 nm.



The characterized material was used to make measurements of the rate of the ammonia catalytic decomposition at conditions of ammonia content at the reactor inlet in the range from 0 to 100%. Results of thermogravimetric measurement and changes of hydrogen content in the gas phase at the reactor outlet as a function of time were plotted in Fig. 7.

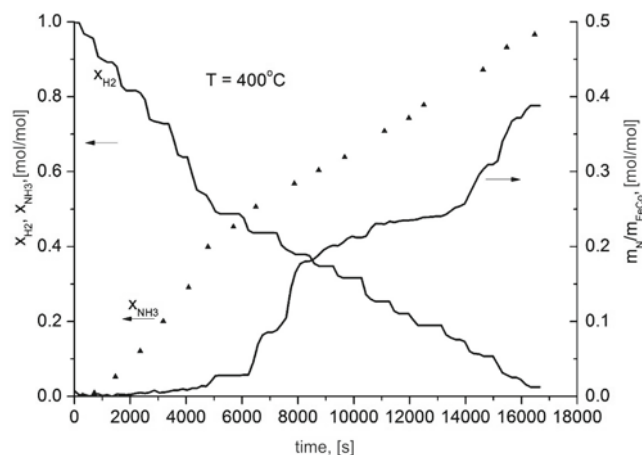


Figure 7. Hydrogen concentration changes and the nitriding degree vs. time at temperature 400°C

Stationary states, in which hydrogen content do not change and the ammonia decomposition rate is constant, settle in about 500 s after a step change in gas mixture feeding the reactor. Catalyst mass change connected with the nitriding process was also observed. It was expressed

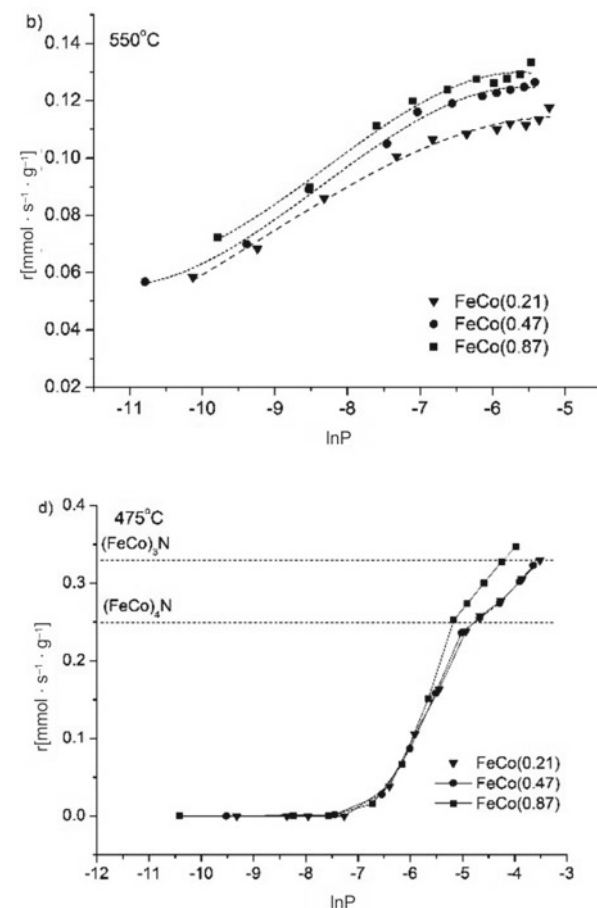


Figure 8. Dependence of the ammonia decomposition rate as a function of nitriding potential ($\ln P = p_{\text{NH}_3}/p_{\text{H}_2}^{1.5}$): a) at 600°C , b) at 550°C , c) at 475°C , d) mass changes of the catalysts during the ammonia decomposition process at 475°C as a function of the logarithm of the nitriding potential

as a ratio of number of moles of nitrogen and number of moles of catalyst. The maximum increase in catalyst mass was registered for ϵ phase.

Changes of the ammonia decomposition reaction rate as a function of logarithm of nitriding potential ($\ln P = p_{\text{NH}_3}/p_{\text{H}_2}^{1.5}$) at temperatures of 600, 550, and 475°C and mass changes of the catalysts during the ammonia decomposition process at 475°C are shown in Figure 8.

Ammonia decomposition rate was calculated from gas phase content in stationary states. At 600°C the rate ammonia decomposition increases while nitriding potential increases. At these conditions mass changes of the catalyst were not observed. At 550°C it was observed that from a value of nitriding potential of about $\ln P = -7$ the ammonia decomposition rate settles at a constant level. Mass change, 0.1 mol N/ mol FeCo, was also observed. At the lower temperature of 475°C, above $\ln P = -7$ a decrease in the reaction rate was registered. Simultaneously a decrease in the reaction rate and an increase in catalyst mass were measured. The dependence of catalyst mass changes as a function of logarithm of nitriding potential was presented in Figure 7d. While ammonia content in the reactor increases catalyst mass increases too. Stoichiometric compositions corresponding to γ' -(FeCo)₄N i ϵ -(FeCo)₃N phases were marked with vertical lines. At the same conditions higher nitriding degree was achieved for the FeCo(0.87) catalyst, which contains more potassium oxide.

Presence of these phases was confirmed with the roentgen diffraction method, Figure 9.

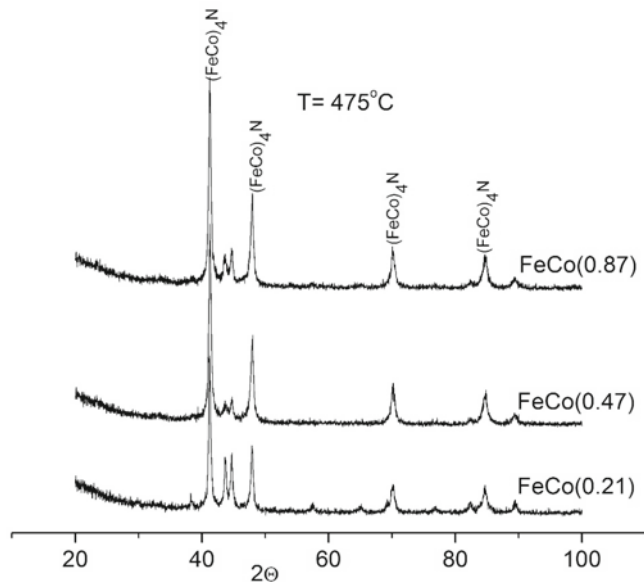


Figure 9. XRD patterns of the catalysts after ammonia decomposition at 475°C

On all X-ray patterns there are visible peaks belonging to γ' -(FeCo)₄N, ϵ -(FeCo)₃N, and solid solution of iron and cobalt phases.

Table 2. Catalytic activities of bimetallic catalysts for the ammonia decomposition at 600°C

Catalyst	GHSV _{NH₃} [ml/g _{cat} h]	NH ₃ conversion [%]	Ref.
FeCo(0.87)	32000	49.0	This work
CoFe ₅ /CNTs	36000	48.0	[17]
Co ₇ Mo ₃ /MCM-41	36000	99.2	[14]

The decomposition degree of the ammonia over FeCo(0.87) catalyst is lower in comparison with bimetallic supported catalysts presented in the literature. Although the advantage of that catalyst is the fact that it is a fused catalyst. The same mass of the catalyst has significantly lower volume in comparison to supported catalysts, and much more higher mechanic resistance.

CONCLUSIONS

Potassium oxide develops specific surface area of the catalyst and increases a number of adsorption sites for hydrogen. An increase in potassium oxide content enhances catalyst activity in the ammonia decomposition reaction. At the temperature of 475°C the nitriding process of the catalyst takes place and a new phase is being formed over which the ammonia decomposition rate decreases.

LITERATURE CITED

- Schlapbach, L. & Züttel, A. (2001). Hydrogen-storage materials for mobile applications. *Nature*. 414, 353–358.
- Chellappa, A.S., Fischer, C.M. & Thomson, W.J. (2002). Ammonia decomposition kinetics over Ni-Pt/Al₂O₃ for PEM fuel cell applications. *Appl. Catal. A*. 227, 231–240.
- Yin, S.F., Zhang, Q.H., Xu, B.Q., Zhu, W.X., Ng, Ch.F. & Au, Ch.T. (2004). Investigation on the catalysis of CO_x-free hydrogen generation from ammonia. *J. Catal.* 224, 384–396. DOI: 10.1016/j.jcat.2004.03.008.
- Yin, S.F., et al. (2004). A mini-review on ammonia decomposition catalysts for on site generation of hydrogen for fuel cell applications. *Appl. Catal. A*. 277, 1–9. DOI: 10.1016/j.apcata.2004.09.020.
- Schuth, F., Palkovits, R., Schlogl, R. & Su, D.S. (2012). Ammonia as a possible element in an energy infrastructure: catalysts for ammonia decomposition. *Energy Environ. Sci.* 5, 6278–6289. DOI: 10.1039/c2ee02865d.
- Lendzion-Bielun, Z., Pelka, R. & Arabczyk, W. (2009). Study of the Kinetics of Ammonia Synthesis and Decomposition on Iron and Cobalt Catalysts. *Catal. Lett.* 129, 119–121. DOI: 10.1007/s10562-008-9785-x.
- Choi, J.G. (2004). Ammonia decomposition over Mo carbide catalysts. *J. Ind. Eng. Chem.* 10, 967–971.
- Choi, J.G. (1999). Ammonia decomposition over vanadium carbide catalysts. *J. Catal.* 182, 104–116.
- Ganley, J.C., Thomas, F.S., Seebauer, E.G. & Masel, R.I. (2004). A priori catalytic activity correlations: the difficult case of hydrogen production from ammonia. *Catal. Lett.* 96, 117–122. DOI: 10.1016/j.cattod.2004.07.000.
- Hansgen, D.A., Vlachos, D.G. & Chen, J.G. (2010). Using First principles to predict bimetallic catalysts for the ammonia decomposition reaction. *Nature Chem.* 2, 484–489. DOI: 10.1038/NCHEM.626.
- Duan, X., Ji, J., Qian, G., Fan, Ch., Zhu, Y., Zhou, X., Chen, D., Yuan, W. (2012). Ammonia decomposition on Fe(111), Co(111) and Ni(111) surfaces: A density functional theory study. *J. Mol. Catal. A: Chem.* 357, 81–86. DOI: 10.1016/j.molcata.2012.01.023.
- Pelka, R., Moszynska, I. & Arabczyk, W. (2009). Catalytic ammonia decomposition over Fe/Fe₄N. *Catal. Lett.* 128, 72–76. DOI: 10.1007/s10562-008-9758-0.
- Lendzion-Bielun, Z. & Arabczyk, W. (2013). Fused FeCo catalysts for hydrogen production by means of the ammonia decomposition reaction. *Catal. Today*. 212, 215–219. DOI: 10.1016/j.cattod.2012.12.014.
- Duan, X., Qian, G., Zhou, X., Chen, D. & Yuan, W. (2012). MCM-41 supported Co-Mo bimetallic catalysts for

enhanced hydrogen production by ammonia decomposition. *Chem. Eng. J.* 207–208, 103–108. DOI: 10.1016/j.cej.2012.05.100.

15. Ji, J., Duan, X., Qian, G., Zhou, X., Tong, G. & Yuan, W. (2014). Towards an efficient CoMo/ γ -Al₂O₃ catalyst using metal amine metallate as an active phase precursor: Enhanced hydrogen production by ammonia decomposition. *Int. J. Hydrogen Energy.* 39, 12490–12498. DOI: 10.1016/j.ijhydene.2014.06.081.

16. Liang, Ch., Li, W., Xin, Q. & Li, C. (2000). Catalytic decomposition of ammonia over nitrated NiMoN_x/ α -Al₂O₃ catalysts. *Ind. Eng. Chem. Res.* 39, 3694–3697. DOI: 10.1021/ie990931n.

17. Zhang, J., Muller, J.-O., Zheng, W., Wang, D., Su, D. & Schlögl, R. (2008). Individual Fe-Co alloy nanoparticles on carbon nanotubes: structural and catalytic properties. *Nano Lett.* 8(9), 2738–2743. DOI: 10.1021/nl8011984.

18. Hill, A.K. & Torrente-Murciano, L. (2014). In-situ H₂ production via low temperature decomposition of ammonia: Insights into the role of cesium as a promoter. *Inter. J. Hydro. Ene.* 39, 7646–7654. DOI: 10.1016/j.ijhydene.2014.03.043.

19. Raróg-Pilecka, W., Szmigiel, D., Kowalczyk, Z., Jodzis, S. & Zielinski, J. (2003). Ammonia decomposition over the carbon-based ruthenium catalyst promoted with barium or cesium. *J. Catal.* 218, 465–469. DOI: 10.1016/S0021-9517(03)00058-7.

20. Pelka, R. & Arabczyk, W. (2013). A new method for determining the nanocrystallite size distribution in systems where chemical reaction between solid and a gas phase occurs. *J. Nanomat.* DOI: 10.1155/2013/645050.